AUT Journal of Civil Engineering

AUT J. Civil Eng., 6(3) (2022) 415-432
DOI: 10.22060/ajce.2023.22297.5824

Effect of Load Eccentricity on the Bearing Capacity of Strip Footings on Rock Masses

A. Erfanian, M. Imani*[2]

[1] Geotechnical Engineering Group, Amirkabir University of Technology, Garmsar Campus, Garmsar, Iran

ABSTRACT: In general, the effect of load eccentricity should be considered in determining the ultimate bearing capacity of foundations. In the present study, the upper bound method of limit analysis was used to propose an equation for determining the bearing capacity of rock masses subjected to the load of a strip footing. The Hoek-Brown failure criterion was used for the rock mass and the footing load was assumed to be exerted eccentrically to the rock mass. The maximum eccentricity value was limited to 1/6 of the footing width to keep the whole footing base in contact with the underneath ground and not result in lifting the footing. Extensive parametric analyses were performed to investigate the effect of the footing width and the rock mass properties on the bearing capacity of rock masses subjected to the eccentric loads. The results show that increasing the load eccentricity from zero to 1/12 and 1/6 of the footing width results in 20% to 40% reduction in the bearing capacity of rock masses, respectively. Also, for all considered eccentricities, the effect of the rock mass unit weight and the footing width and also the Hoek-Brown parameters σci and mi on the bearing capacity were reduced by increasing GSI. Increasing the unit weight of the rock mass from 20 kN/m3 to 25 kN/m3 results in increasing the bearing capacity between zero and 15%. Also, by increasing the footing width from 1 to 5 meters, the bearing capacity increases between 13% and 46%.

Review History:

Received: Mar. 27, 2023
Revised: May, 24, 2023
Accepted: Jun. 13, 2023
Available Online: Jun. 19, 2023

Keywords:

Load Eccentricity
Bearing Capacity
Strip Footing
Rock Mass
Upper Bound

1- Introduction

A crucial step in foundation design is the determination of the bearing capacity. Foundations might be subjected to eccentric loads from the columns or a combination of centric axial load and bending moments which the bearing capacity of the latter case can be investigated in the same manner as footing subjected to eccentric load without bending moment. Meyerhof [1] conducted preliminary investigations on the bearing capacity of footings subjected to eccentric loads. He considered the effect of eccentricity by introducing the method of dimension reduction. In another study, Meyerhof [2] proposed that the bearing capacity under an eccentric load can be obtained as the bearing capacity of the foundation subjected to the centric load multiplied by a reduction factor.

The finite difference method was applied to investigate the bearing capacity of ring footings on non-cohesive soils under eccentric loads [3]. They proposed a reduction factor that depends on the value of eccentricity and the external and internal diameters of the ring footings. Multiplying the reduction factor by the bearing capacity in the absence of eccentricity results in the eccentric ultimate bearing capacity.

In another research, the finite element method was used to consider the effect of load eccentricity on the bearing capacity of a strip footing located in the vicinity of a slope [4]. Also, several experiments were conducted to determine the bearing capacity of footings rested on sand subjected to eccentric loads [5]. He considered three values for the eccentricity of the footing load concerning the footing center which includes *B*/24, *B*/16, and *B*/12 (*B* is the footing width). The effect of load eccentricity on the bearing capacity of circular, rectangular, and strip footings on loose sandy soils was also investigated [6]. Moreover, the limit equilibrium method was applied to investigate the bearing capacity of strip footings under eccentric and oblique loads [7]. The results of this research were presented as bearing capacity coefficients which depend on the internal friction angle of the soil, the ratio of load eccentricity to the foundation width, and the applied vertical load. In another study, a neural network technique was used to examine the effects of load eccentricity and inclination, soil internal friction angle, and the footing width and embedment depth on the bearing capacity of strip footings [8].

The bearing capacity of rock masses has been focused on in recent years by researchers and different subjects were studied including the bearing capacity subjected to axial centric loads [9-13], groundwater [14, 15], adjacent footings [16-18], seepage [19, 20] and the footing embedment depth [21, 22]. To the authors' knowledge, the effect of load eccentricity on the bearing capacity of rock masses is an issue with minor focus from researchers. However, this is a vital

*Corresponding author's email: imani@aut.ac.ir

topic for the rock foundation of large structures, like bridges, which impose eccentric loads on the ground on which they are founded.

Among few studies regarding the bearing capacity of rock masses subjected to eccentric loads, one can mention the method presented by Keawsawasvong et al. [23]. By using the Optum G2 software and applying the Hoek-Brown failure criterion, they showed that increasing the load eccentricity results in decreasing the bearing capacity. Regarding the limitation of conducted studies about the bearing capacity of rock masses under eccentric loads and considering the significant application of the Hoek-Brown failure criterion in practical problems of rock masses, this research has focused on developing a formulation for the ultimate bearing capacity of rock masses under eccentric loads. The equations proposed in this paper are based on the upper bound method of limit analysis which is well-known in bearing capacity calculations. Because of the eccentricity of the load applied to the footing, an asymmetrical failure mechanism was considered for the analyses since the maximum eccentricity for which, the footing is fully in contact with the ground is 1/6 of the footing width, the maximum eccentricity considered in this study as limited to 1/6 of the footing width. Finally, parametric analyses were conducted to determine the effect of different rock mass properties on the bearing capacity under eccentric loads

.

2- Using the upper bound method for rock masses following the modified Hoek-Brown criterion

Comparing to the Mohr-Coulomb failure criterion which was used in some previous researches [24]{Yousefian, 2020 #1}, the Hoek-Brown criterion is widely used in practical problems as the most common rock mass failure criterion [25]. The general form of this criterion is shown in Eq. (1):

$$\sigma_1' = \sigma_3' + \sigma_{ci}\left(m\frac{\sigma_3'}{\sigma_{ci}} + s\right)^a \tag{1}$$

Where σ'_1 and σ'_3 are the major and minor effective principal stresses, respectively, and σ_{ci} is the uniaxial compressive strength of the intact rock. m, s and a can be obtained as follows:

$$m = m_i \exp\left(\frac{GSI-100}{28-14D}\right) \tag{2}$$

$$s = \exp\left(\frac{GSI-100}{9-3D}\right) \tag{3}$$

$$a = \frac{1}{2} + \frac{1}{6}\left(e^{\frac{-GSI}{15}} - e^{\frac{-20}{3}}\right) \tag{4}$$

where m_i is a constant that varies from 5 to 33. GSI refers to the geological strength index of the rock mass and D is the disturbance factor which ranges from zero to one.

As explained in the following sections, having shear strength parameters of the material, *i.e.*, cohesion (c) and friction angle (ϕ), is necessary for upper bound calculations [26]. However, there is no direct access to these parameters in the Hoek-Brown criterion. Yang and Yin [13] proposed that the non-linear Hoek-Brown criterion be replaced by a tangential straight line, where the angle of this line with the horizon was introduced as ϕ_t (the angle of internal friction), and its vertical intercept was named as c_t (tangential cohesion).

$$\tau = c_t + \sigma_n \tan\phi_t \tag{5}$$

The location of this tangential line with respect to the non-linear Hoek-Brown criterion should be determined through an optimization technique to achieve the lowest possible bearing capacity which means that ϕ_t should be incorporated in the bearing capacity equation as an unknown parameter [13]. After determining it through the optimization, the corresponding c_t can be obtained as follows:

$$\frac{c_t}{\sigma_{ci}} = \frac{\cos\phi_t}{2}\left[\frac{ma\left(1-\sin\phi_t\right)}{2\sin\phi_t}\right]^{\frac{a}{1-a}} - \frac{\tan\phi_t}{m}\left(1+\frac{\sin\phi_t}{a}\right)\left[\frac{ma\left(1-\sin\phi_t\right)}{2\sin\phi_t}\right]^{\frac{1}{1-a}} + \frac{s}{m}\tan\phi_t \tag{6}$$

replacing the non-linear Hoek-Brown criterion with a single straight line does not deliver precise results. For overcoming this approximation, Mao et al. [27] proposed the multi-tangential techniques shown in Fig. 1. In this method, the original non-linear Hoek-Brown criterion is replaced by several tangential lines, each of them has a unique angle with the horizon (ϕ_{ti}) and the vertical intercept (c_{ti}). Therefore, several unknown ϕ_{ti} angles are entered into the analyses which should be determined through an optimization technique. After determining them, the corresponding c_{ti} values can be obtained using Eq. 6. Although this method results in increasing the analysis time, it improves the accuracy of the bearing capacity considerably [18, 19, 22]. This method was employed for the first time in this paper to obtain the effect of load eccentricity on the bearing capacity of rock masses.

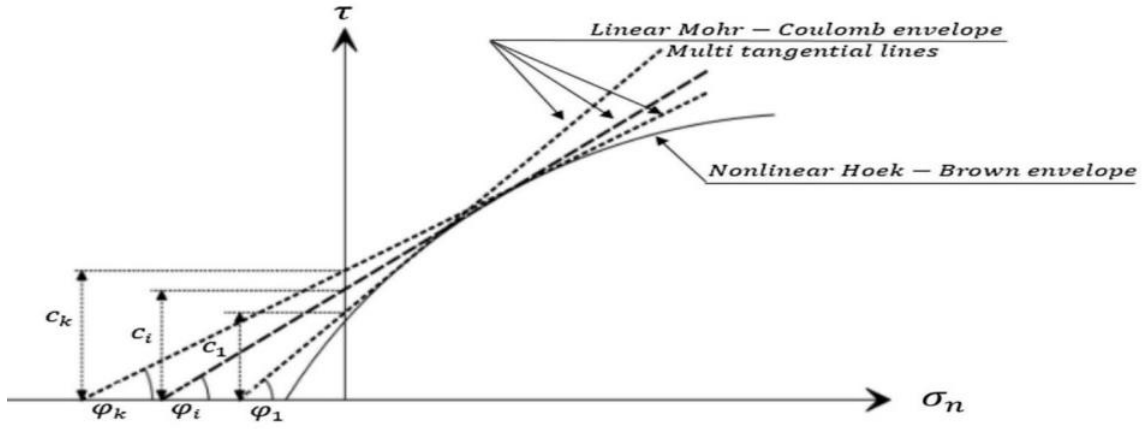

Fig. 1. The multi-tangential linearization approach [27]

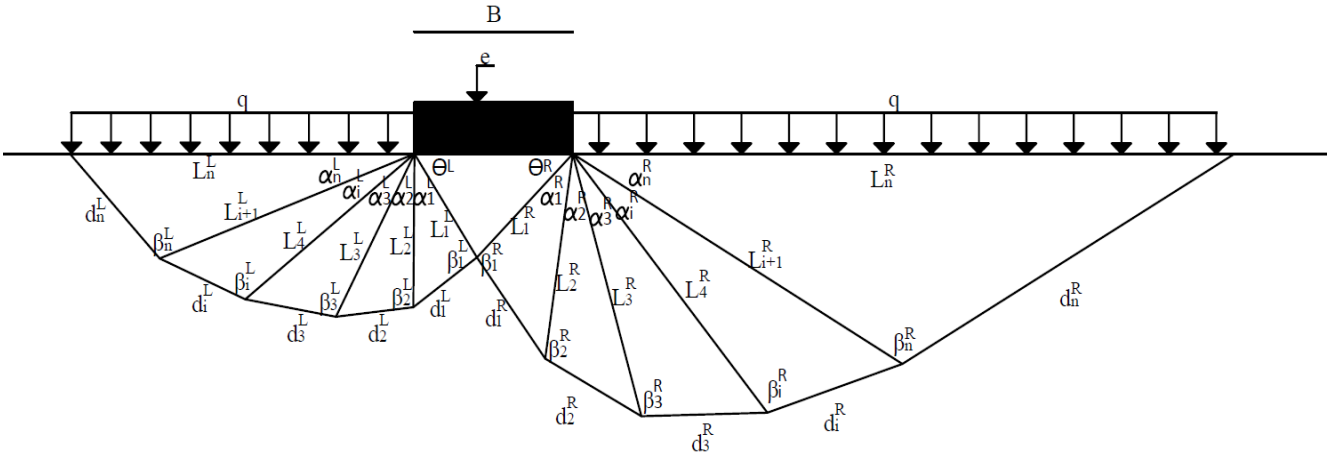

Fig. 2. The failure mechanism considered in the present paper

3- Determining the bearing capacity of rock masses under eccentric loads

3- 1- The failure mechanism

Because of the eccentricity of the footing load, a non-symmetric failure mechanism was considered in the present paper, as shown in Fig. 2. The mechanism consists of a central triangular wedge beneath the footing and *m* and *n* triangular wedges in the right and left sides of the central wedge, respectively. The eccentricity of the load is equal to *e* with respect to the footing centerline. The surcharge *q* was considered to be applied to the sides of the footing. It was assumed that the apex of the central triangular wedge beneath the footing lies along the load applied to the footing. L_i^L, L_i^R, d_i^L, and d_i^R are the length of the velocity discontinuity lines. The angles θ^L, θ^R, α_i^L, α_i^R, β_i^L, and β_i^R are unknowns, and their value should be determined by optimization of the bearing capacity formula developed in this paper in such a way that the lowest possible bearing capacity be achieved. Fig. 3 shows the velocity field and the corresponding hodograph. V_i^L, and V_i^R are the velocity of each triangular wedge, and $V^L_{i-1,i}$, and $V^R_{i-1,i}$ are the relative velocity between two adjacent wedges. The angle between each velocity vector and the corresponding velocity discontinuity line is equal to the internal friction angle of the rock mass [26]. As explained previously, since the multi-tangential technique was applied in this paper, the angle between each velocity vector and the corresponding discontinuity line (ϕ_i^L, ϕ_i^R, $\phi_{i-1,i}{}^L$ and $\phi_{i-1,i}{}^R$) is unique and unknown, which should be determined through optimization.

3- 2- The length of velocity discontinuity lines and the area of the wedges

For conducting upper bound calculations, the length of velocity discontinuity lines and the area of the wedges should be determined. The procedure for the determination of these parameters were presented in the appendix.

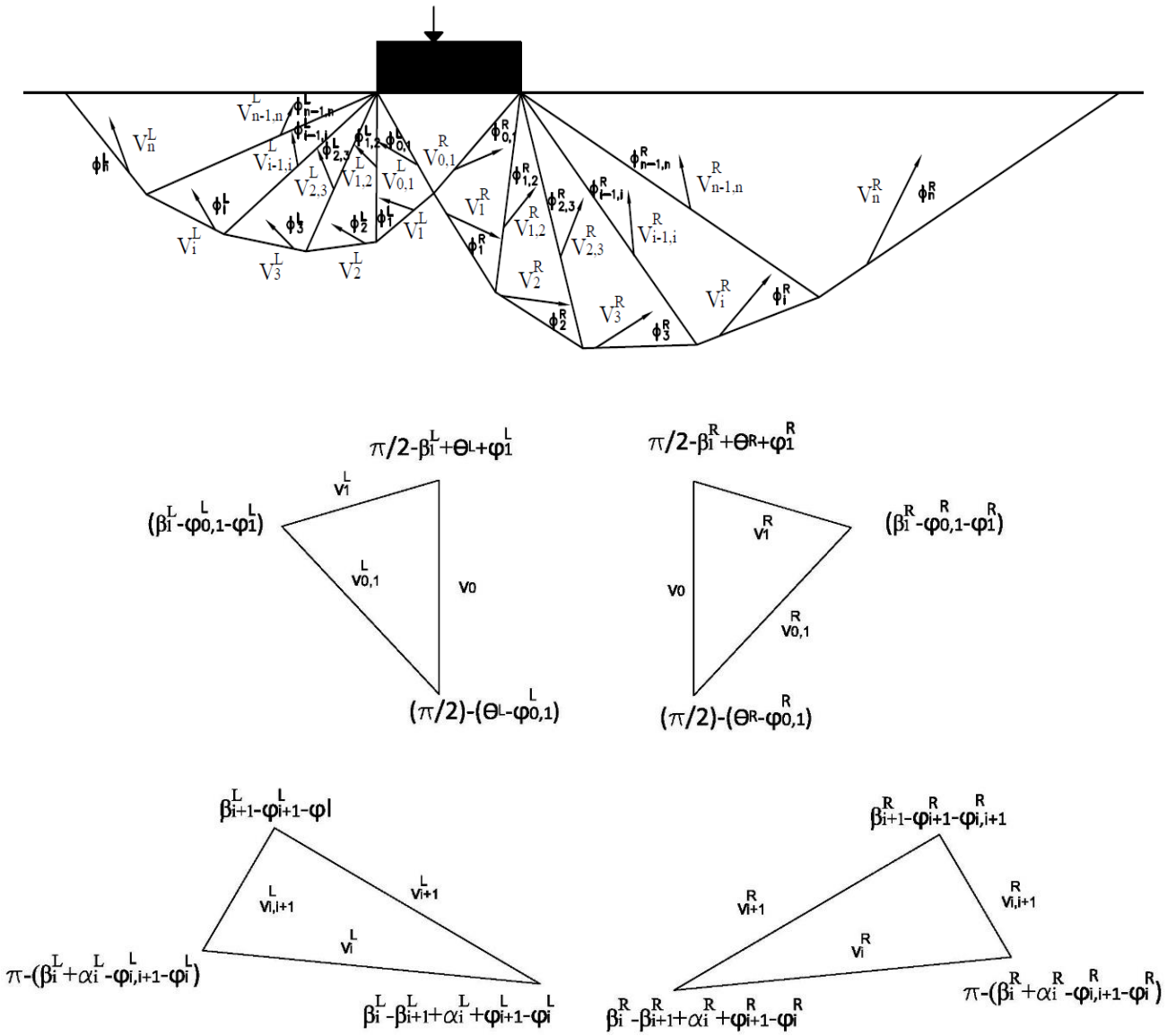

Fig. 3. The velocity field and the corresponding hodograph

3- 3- Internal energy dissipation and external work

The total amount of the internal energy dissipated in the mechanism is equal to the sum of the energy dissipated along the velocity discontinuity lines which in turn, is equal to the length of each discontinuity line multiplied by the velocity and the cohesion along it. Also, the total amount of the external work exerted on the mechanism is equal to the sum of the external work due to the weight of wedges (W_γ), the footing load (W_{que}), and the surcharge (W_q). The calculation procedure was presented in the appendix.

3- 4- Ultimate bearing capacity of rock masses subjected to eccentric loads

By equating the internal energy dissipated in the mechanism (Eq. A9) to the external work exerted by the mechanism (Eq. A19), the general formula for the ultimate bearing capacity of rock masses under the eccentric loads of strip footings was obtained as follows:

$$q_{ue} = s^{0.5}\sigma_{ci}N_{\sigma e} + qN_{qe} + 0.5\gamma BN_{\gamma e} \tag{7}$$

Where $N_{\sigma e}$, N_{qe}, and $N_{\gamma e}$ are the bearing capacity factors which are:

$$N_{\sigma e} = f_1^R + f_2^R + f_3^R + f_1^L + f_2^L + f_3^L \tag{8}$$

$$N_{qe} = f_4^R + f_4^L \tag{9}$$

$$N_{\gamma e} = f_5^R + f_6^R + f_5^L + f_6^L \tag{10}$$

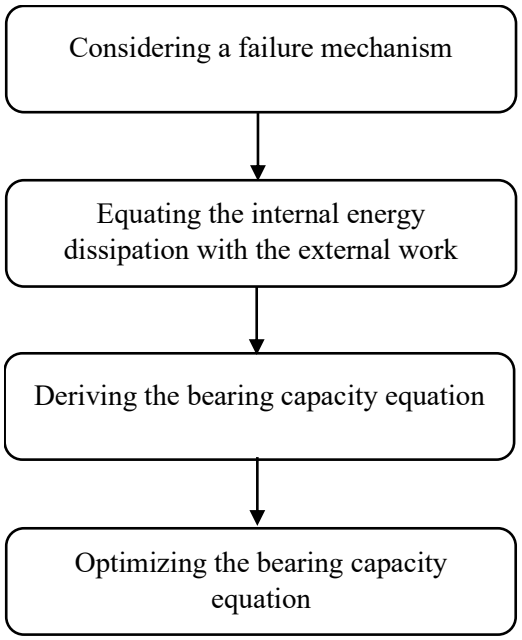

Fig. 4. The flowchart of the solution proposed in this study

3- 5- Optimization of the bearing capacity formula

As mentioned in previous sections, the proposed formula for the bearing capacity of rock masses under eccentric loads contains $4n+4m+2$ unknowns including θ^L, θ^R, α_i^L, α_i^R, β_i^L, β_i^R, ϕ_i^L, ϕ_i^R, $\phi_{i\text{-}1,i}^{\ L}$, and $\phi_{i\text{-}1,i}^{\ R}$. These unknowns should be determined using an optimization technique in such a way that the best (lowest) possible magnitude for the bearing capacity be achieved. n and m are the numbers of triangular wedges on the right and left sides of the central wedge, respectively. The optimization was conducted using the genetic algorithm tool provided in MATLAB software. For the assumed failure mechanism to be kinematically admissible, the unknown parameters were constrained appropriately to avoid unrealistic values. Based on the geometry of the failure mechanism and the velocity hodograph, the following constraints were considered:

$$\begin{aligned}
&\alpha_i^R+\beta_i^R=\pi \quad , \quad \sum\alpha_i^R+\theta^R=\pi \quad , \quad \phi_{i+1}^R+\phi_{i-1,i}^R-\beta_{i+1}^R<0\\
&0<\alpha_i^R+\beta_i^R-\beta_{i+1}^R-\phi_i^R+\phi_{i+1}^R<\pi \quad , \quad \beta_1^R-\theta^R-\phi_1^R<\frac{\pi}{2}\\
&\alpha_i^L+\beta_i^L=\pi \quad , \quad \sum\alpha_i^L+\theta^L=\pi \quad , \quad \phi_{i+1}^L+\phi_{i-1,i}^L-\beta_{i+1}^L<0\\
&0<\alpha_i^L+\beta_i^L-\beta_{i+1}^L-\phi_i^L+\phi_{i+1}^L<\pi \quad , \quad \beta_1^L-\theta^L-\phi_1^L<\frac{\pi}{2}\\
&0<\theta^R,\theta^L<\frac{\pi}{2} \quad , \quad 0<\alpha_i^R,\alpha_i^L<\frac{\pi}{2} \quad , \quad 0<\beta_i^R,\beta_i^L<\pi\\
&0<\phi_i^R,\phi_i^L,\phi_{i+1}^R,\phi_{i+1}^L,<\frac{\pi}{2}
\end{aligned} \tag{11}$$

Fig. 4 Shows a flowchart for the procedure of the solution proposed in this study.

4- Comparison of the results with other available methods

The formula proposed for the bearing capacity (Eq. 7) comprises three parts which depend on σ_{ci}, q and γ. Since the magnitude of σ_{ci} is commonly high in rock masses, the effect of the first part of Eq. 7, i.e., $s^{0.5}\sigma_{ci}N_{\sigma e}$, is larger than the share of the two next parts, i.e., qN_{qe} and $0.5\gamma BN_{\gamma e}$. Therefore, in most previous studies, by ignoring the effect of q and γ, the general form of the bearing capacity of rock masses reduced into the following form [10, 13, 18, 19, 28]:

$$q_{ue}=s^{0.5}\sigma_{ci}N_{\sigma e} \tag{12}$$

Therefore, the bearing capacity factor $N_{\sigma e}$ is:

$$N_{\sigma e}=\frac{q_{ue}}{s^{0.5}\sigma_{ci}} \tag{13}$$

By using this dimensionless factor, some comparisons with other available solutions were performed in the following sections to show the reliability of the proposed formulation in the current study.

4- 1- Determining the optimal number of wedges

As mentioned before, n and m wedges were considered on the right and left sides of the central wedge, respectively. For determining the optimal values of n and m, different values of these parameters were considered. For simplicity, n and m were assumed to be equal to each other. Table 1 presents the magnitude of $N_{\sigma e}$ for different values of $n = m$. it is clear that by increasing $n = m$, the difference between two successive

Table 1. Variation of $N_{\sigma e}$ versus n=m assuming σ_{ci}=10 MPa, m_i=7, GSI=50, D=0 and B=1 m

$n = m$	$e = 0$		$e = B/12$		$e = B/6$	
	$N_{\sigma e}$	Reduction (%)	$N_{\sigma e}$	Reduction (%)	$N_{\sigma e}$	Reduction (%)
2	11.468	-	9.403	-	6.880	-
3	10.087	13.7	8.069	14.2	6.169	10.3
4	9.284	8.7	7.248	10.2	5.689	8.4
5	8.823	5.2	6.753	6.8	5.490	3.5
6	8.428	4.7	6.658	1.4	5.326	3
7	8.296	1.59	6.603	0.8	5.186	2.6
8	8.277	0.23	6.539	0.97	5.154	0.62
9	8.269	0.1	6.515	0.37	5.135	0.37

Table 2. Comparison among the $N_{\sigma e}$ obtained from different methods

GSI	Present study	AlKhafaji et al.[19]	Difference (%)	Saada et al.[10]	Difference (%)	Yang & Yin [13]	Difference (%)
10	19.376	18.518	4.4	19.546	5.6	49.160	165.5
30	26.595	26.191	1.5	30.369	16	67.081	156.1
50	19.762	19.472	1.5	25.067	28.7	49.835	155.9
70	14.012	13.878	1.0	18.891	36.1	34.159	146.1
90	10.079	9.95	1.3	-	-	-	-

n=m reduces. For $n = m = 9$, the difference becomes smaller than 0.5%. Therefore, the analyses considered in this study were performed assuming $n = m = 9$.

4- 2- The case of footing load without eccentricity

By putting e=0 in the bearing capacity formula proposed in the current paper, the bearing capacity for the case of centric loads can be obtained. Therefore, the results of the present paper can be compared with the available methods for the case of the rock masses subjected to vertical load without eccentricity. Assuming σ_{ci}=10 MPa, m_i=17, D=0, B=1m, and e=0, Table 2 presents a comparison among different methods. A substantial agreement between the results of the present method and the method of AlKhafaji et al. [19] can be seen which is due to the similarity between the linearization of the Hoek-Brown criterion in these two methods, *i.e.*, the multi-tangential technique. There is also a reasonable agreement between the results of the present method and the method of Saada et al. [10], especially for small values of GSI. But the differences between the results of the present study and the Yang and Yin [13] method are significant. As stated previously, Yang and Yin [13] linearized the non-linear Hoek-Brown criterion with a single straight line which results in decreasing the accuracy of their method concerning the multi-tangential technique used in the current paper. Previous studies were also shown an improvement in the results obtained from the multi-tangential technique compared to the Yang and Yin [13] single-line approximation method [10, 18, 19, 22].

4- 3- The case of footing load with eccentricity

The results of the present paper were compared with the method of Keawsawasvong et al. [23] for the case of e >0. It was assumed that σ_{ci}=10 MPa, m_i=10, D=0, and B=1 m. As presented in Table 3, the present method results in smaller $N_{\sigma e}$ (and the corresponding q_{ue}) than the Keawsawasvong et al. [23] method which shows the efficiency of the proposed formulation and the considered optimization technique. As stated before, obtaining a smaller bearing capacity is more valuable in the framework of the upper bound method.

Table 3. Comparison between the $N_{\sigma e}$ obtained from different solutions

GSI	e	Present study	Keawsawasvong et al. [23]	Difference (%)
30	0	14.141	19.151	35.4
	B/12	11.536	15.63	35.5
	B/6	8.593	12.2	42
50	0	11.925	16.56	38.9
	B/12	9.659	13.189	36.5
	B/6	7.512	9.95	32.5
70	0	8.643	13.23	53.1
	B/12	6.827	10.58	55
	B/6	5.179	7.94	53.3

Table 4. Comparison between the $N_{\sigma e}$ obtained from the present study and the finite difference method

e	Present study	Finite Difference Method	Difference (%)
0	14.14	19.06	34.8
B/12	11.54	15.06	30.5
B/6	8.59	11.81	37.5

4- 4- Comparison with numerical models

The results of the present paper were compared with the finite difference-based code, FLAC 2D. Considering σ_{ci}=10 MPa, m_i=10, GSI=30, D=0 and B=1 m, Table 4 presents the comparison between the $N_{\sigma e}$ obtained from the two methods. The present method results in smaller $N_{\sigma e}$ (and the corresponding q_{ue}) than the finite difference method which shows the efficiency of the proposed formulation and the considered optimization technique.

5- Parametric analyses

5- 1- Effect of the load eccentricity (e)

As stated previously, the maximum load eccentricity considered in the present paper is equal to 1/6 of the footing width (e=0.16B). Assuming σ_{ci}=10 MPa, D=0, and B=1 m, and ignoring the effect of the rock mass unit weight and surcharges, the variation of $N_{\sigma e}$ versus e/B is shown in Fig. 5. By increasing the load eccentricity, $N_{\sigma e}$, and the corresponding bearing capacity decreases. By increasing e from zero to B/6 (e=0.16B), the $N_{\sigma e}$ reduces in the range of 37.4% to 42.1% depending on the m_i and GSI magnitudes.

5- 2- Effect of σ_{ci}

Fig. 6 shows the variation of $N_{\sigma e}$ versus σ_{ci} for different values of eccentricity. It was assumed that GSI=10, B=1 m, and D=0, and the effects of the rock mass unit weight and the surcharge were ignored. For m_i=7 and 17, by increasing σ_{ci} from 2 to 10 MPa, $N_{\sigma e}$ reduces about 38.5% and 10.5%, respectively. However, by raising σ_{ci} from 10 to 50 MPa, the maximum reduction of $N_{\sigma e}$ is 8% and 5.3%, respectively. Therefore, by increasing m_i, the effect of σ_{ci} on $N_{\sigma e}$ reduces. Also, by increasing σ_{ci}, the reduction rate of $N_{\sigma e}$ decreases. Note that this reduction of $N_{\sigma e}$ does not result in decreasing the ultimate bearing capacity, since according to Eq. (12), the ultimate bearing capacity is obtained from the product of $N_{\sigma e}$ and σ_{ci}. Thus, despite the reduction of $N_{\sigma e}$, a rise in σ_{ci} results in increasing the ultimate bearing capacity. Comparing the curves related to different values of e show that there is no significant difference among them. Therefore, the load eccentricity does not affect the dependency $N_{\sigma e}$ of to σ_{ci}. It should be mentioned that more analyses were performed using different values of GSI and similar variation trends for $N_{\sigma e}$ versus σ_{ci} were observed.

5- 3- Effect of m_i

Considering GSI=10, D=0, B=1 m and ignoring the rock mass unit weight and the surcharges, Fig. 7 shows the variation of $N_{\sigma e}$ versus m_i for different values of load eccentricity. By increasing m_i from 7 to 25, the $N_{\sigma e}$ experiences an increase between 388% to 397% for the case of σ_{ci}=10 MPa and 188% to 197% for σ_{ci}=70 MPa, depending on the magnitude of e. For smaller values of load eccentricity, $N_{\sigma e}$ was more affected by m_i.

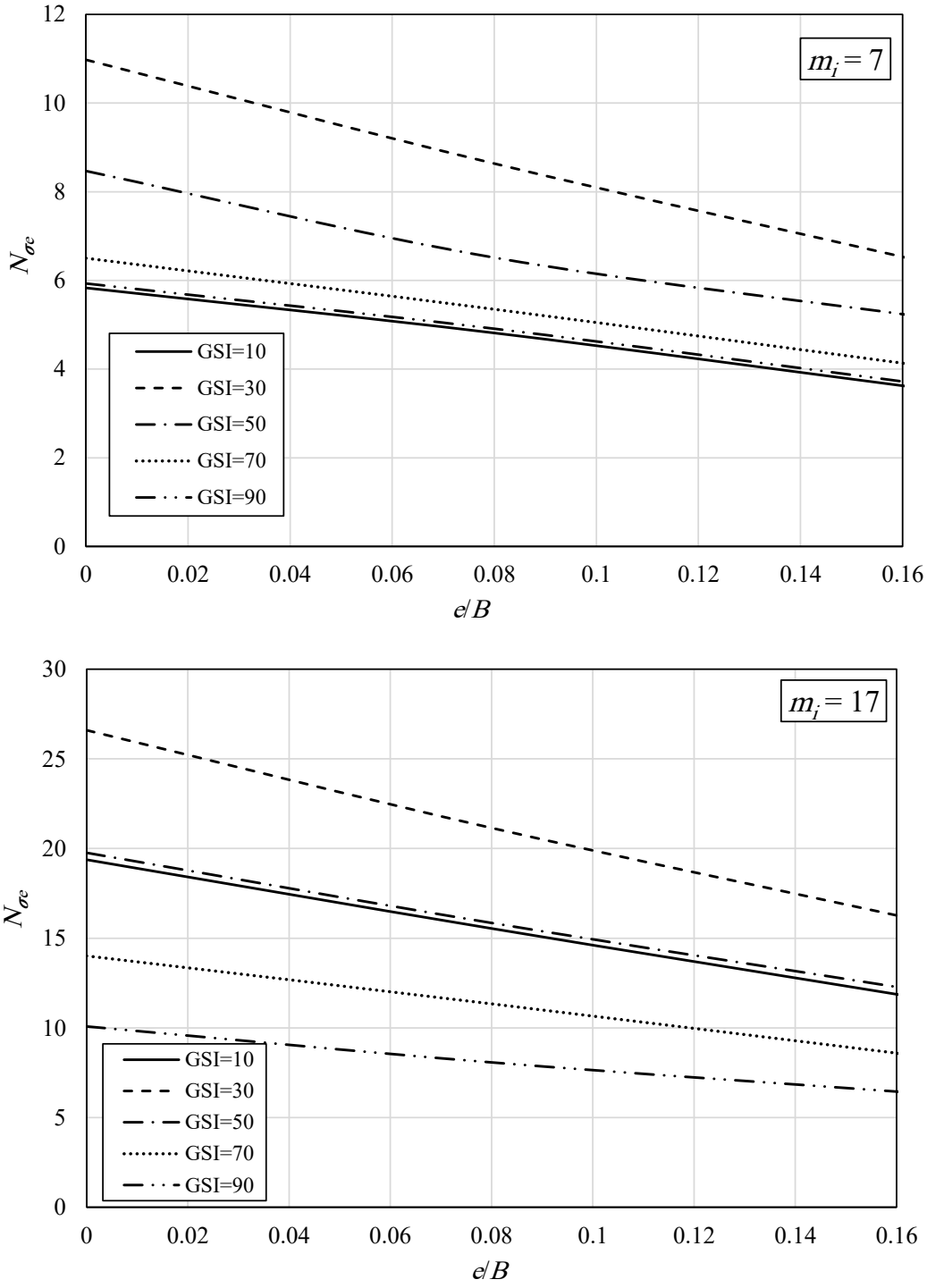

Fig. 5. Variation of $N_{\sigma e}$ versus e/B

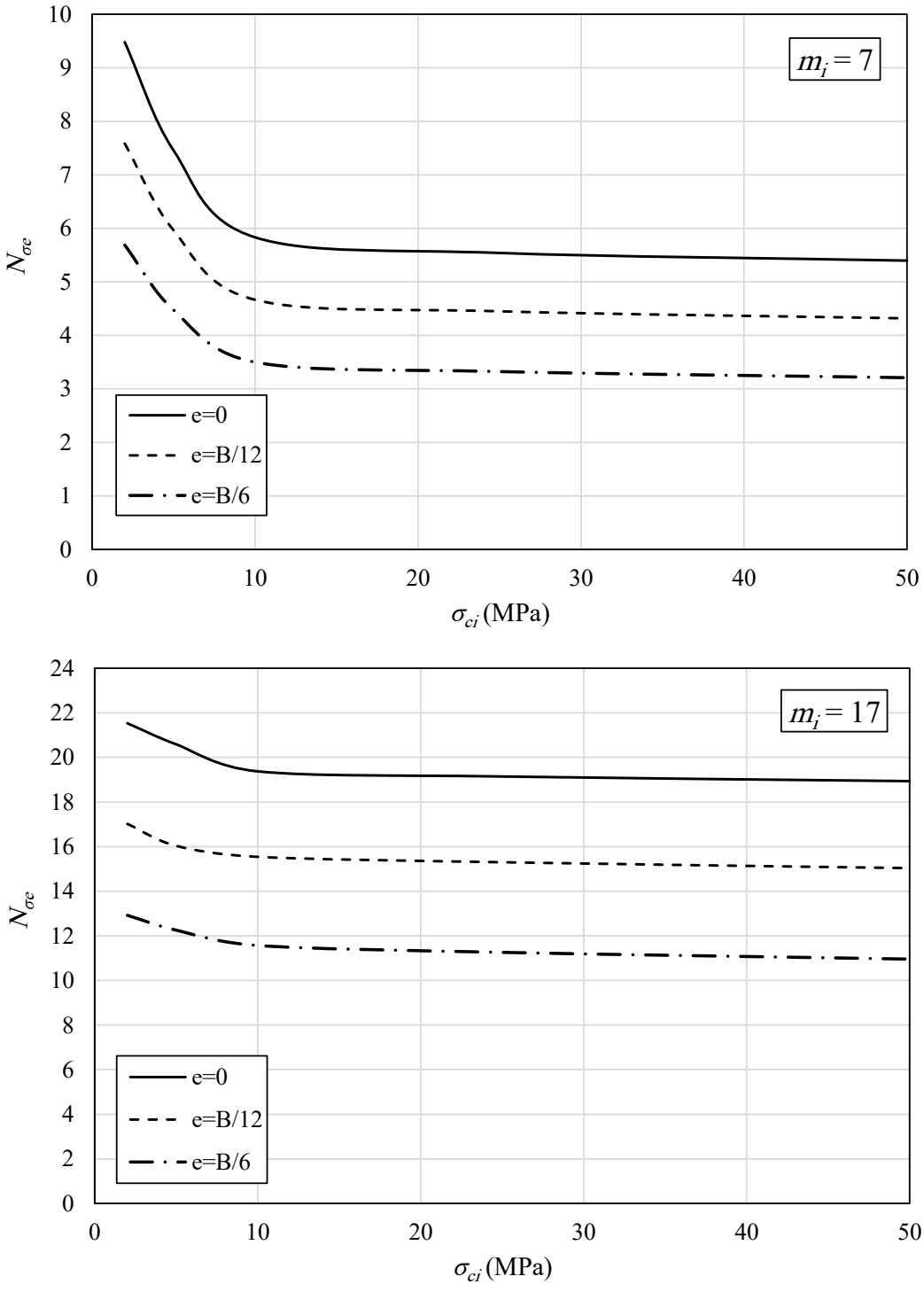

Fig. 6. Variation of $N_{\sigma e}$ versus σ_{ci}

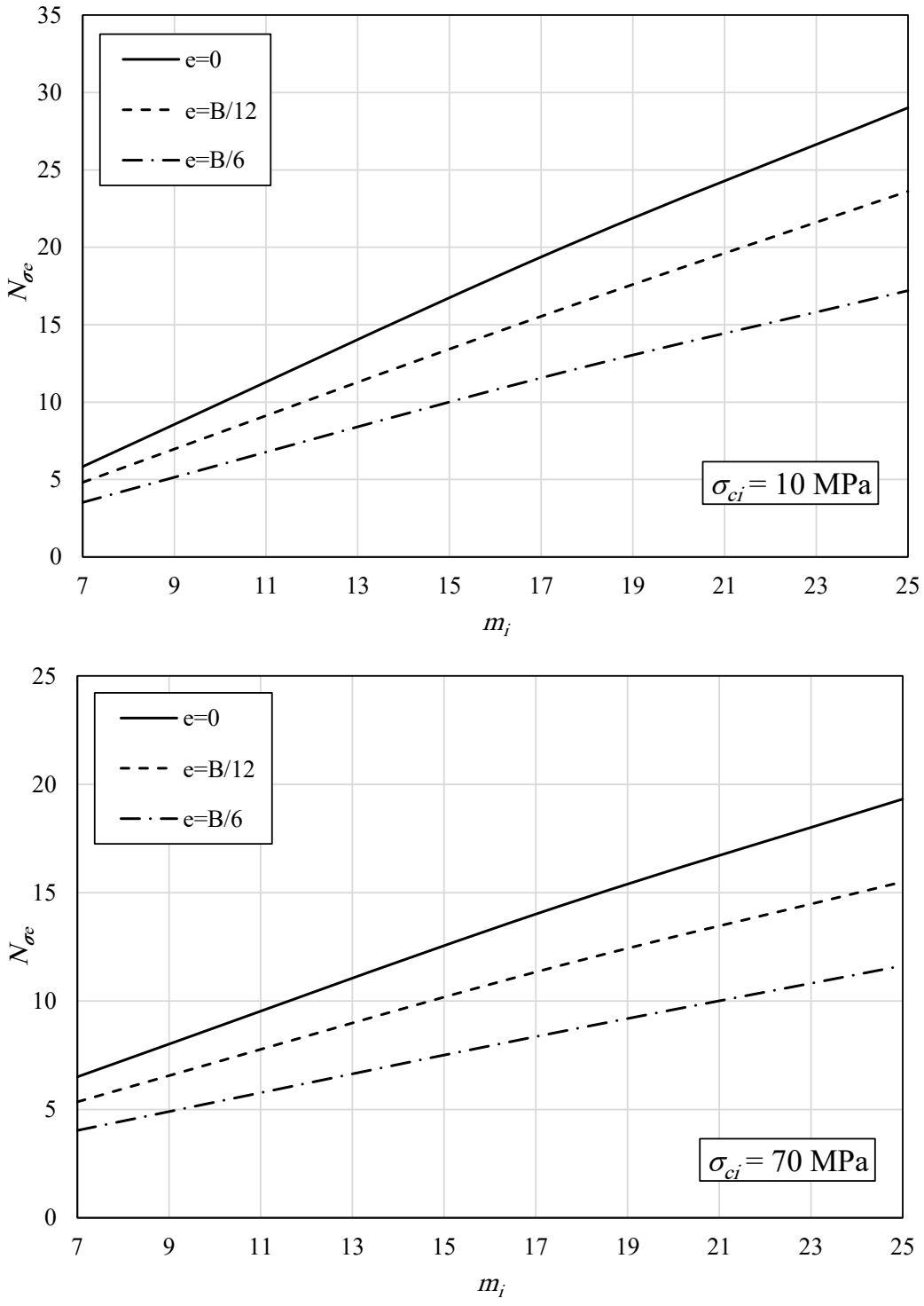

Fig. 7. Variation of $N_{\sigma e}$ versus mi

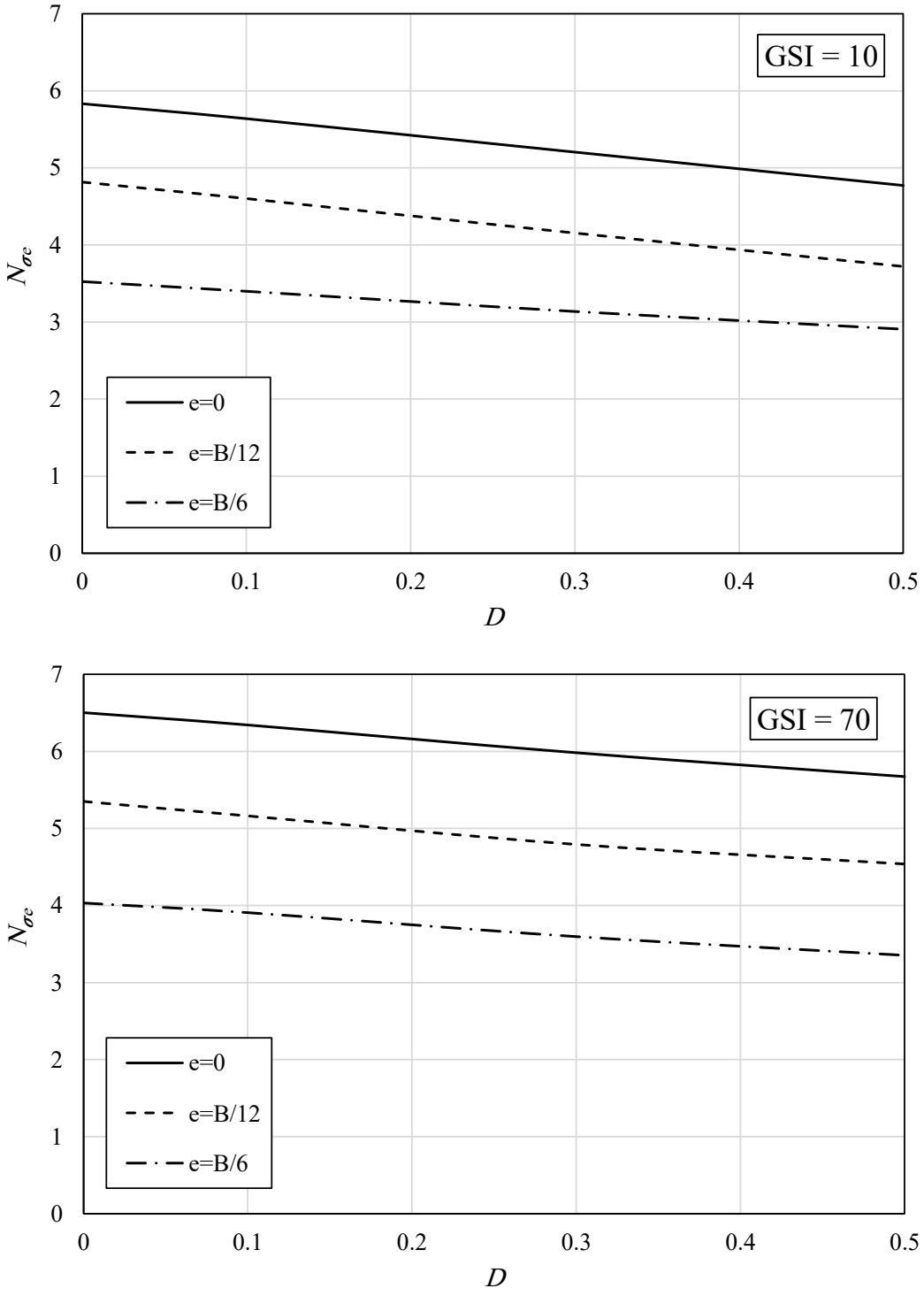

Fig. 8. Variation of $N_{\sigma e}$ versus D

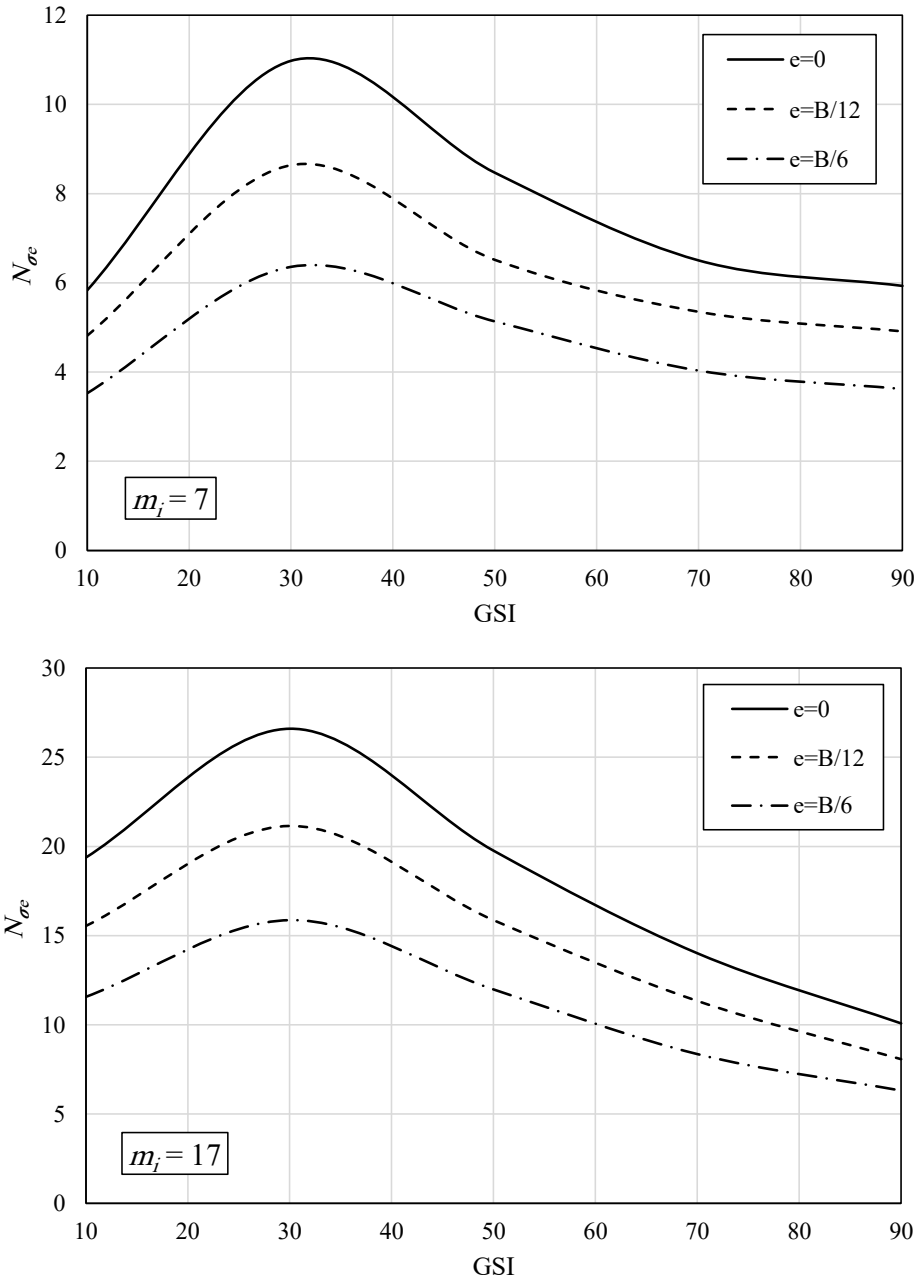

Fig. 9. Variation of $N_{\sigma e}$ versus GSI

5- 4- Effect of *D*

No considerable disturbance imposes on rock masses during preparation as being the foundation for structures. Therefore, assuming D=0 in rock foundation problems is reasonable [11]. However, the effect of other values of D on the effect of load eccentricity on the bearing capacity of rock masses was investigated herein. Considering σ_{ci}=10 MPa, m_i=7, B=1 m and ignoring the effect of the rock mass unit weight and surcharges, Fig. 8 shows the variation of $N_{\sigma e}$ versus D for different values of e and GSI. It is clear that by increasing D from zero to 0.5, the maximum reduction of $N_{\sigma e}$ for GSI=10 and 70 are 22.7% and 16.8%, respectively. However, the value of e does not affect the dependency of $N_{\sigma e}$ to D considerably. For e=0, the maximum reduction of $N_{\sigma e}$ due to increasing D from zero to 0.5 is equal to 18.2%, while for e=B/6, this reduction is about 17.5%.

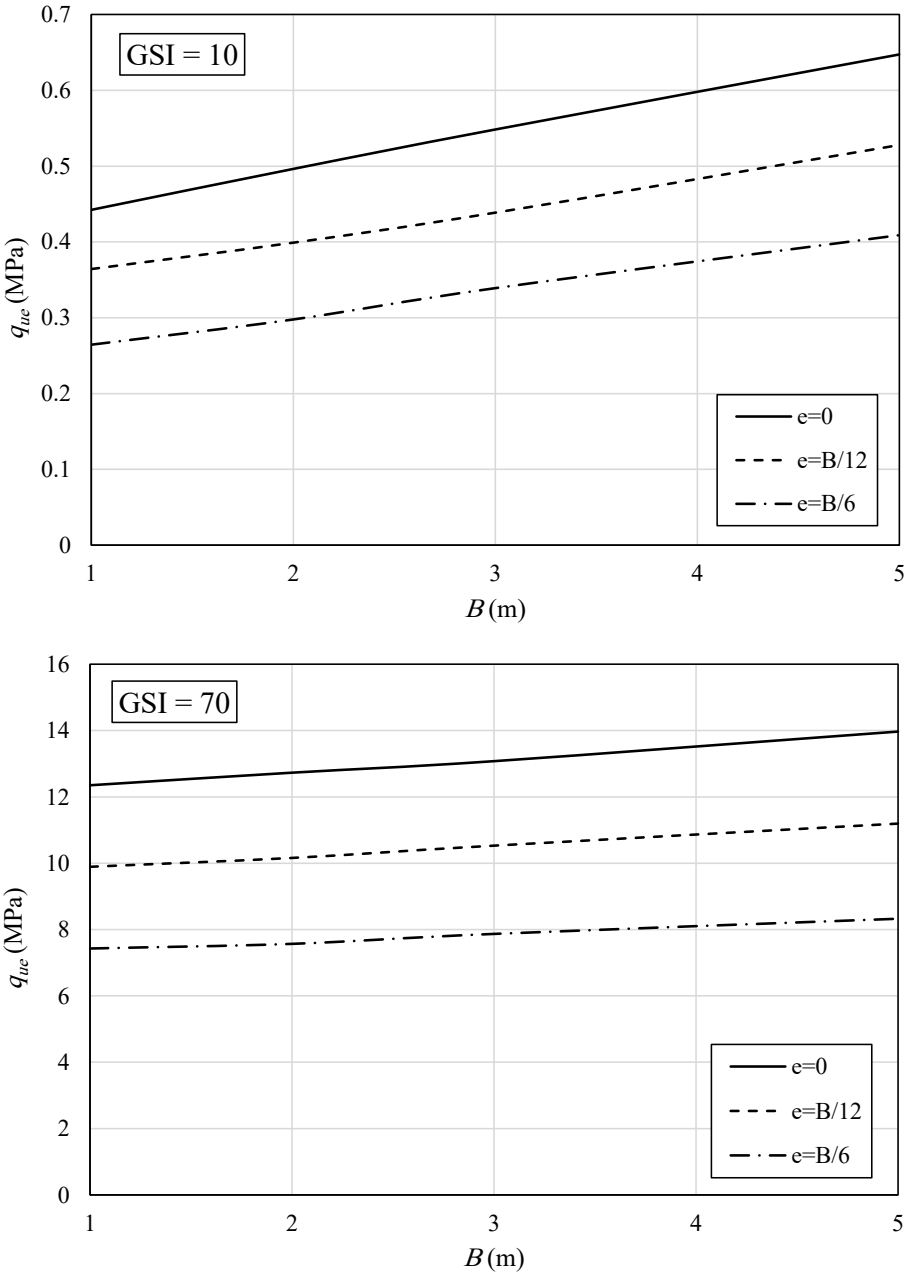

Fig. 10. Variation of q_{ue} versus B

5- 5- Effect of GSI

Fig. 9 shows the variation of $N_{\sigma e}$ versus GSI assuming σ_{ci}=10 MPa and B=1 m. The effect of the rock mass unit weight and the surcharge were ignored. A similar trend of variation of $N_{\sigma e}$ can be seen for different values of e.

5- 6- Effect of the footing width (B)

According to Eq. 7, the bearing capacity depends on the footing width. For investigating the effect of the footing width on the bearing capacity and by ignoring the surcharges, Eq. 7 turns into the following form:

$$q_{ue} = s^{0.5}\sigma_{ci}N_{\sigma e} + 0.5\gamma BN_{\gamma e} \quad (14)$$

Assuming σ_{ci}=10 MPa, m_i=7, D=0, and γ=21 kN/m^3, Fig. 10 illustrates the variation of q_{ue} versus B. In the case of GSI=10 and 70, increasing the footing width from 1 to 5 meters results in a maximum increase in the ultimate bearing capacity of about 54.7% and 13.1%, respectively. Therefore, it can be concluded that the effect of B on the bearing capacity is more sensible for small values of GSI. The eccentricity magnitude does not have a considerable effect on this variation.

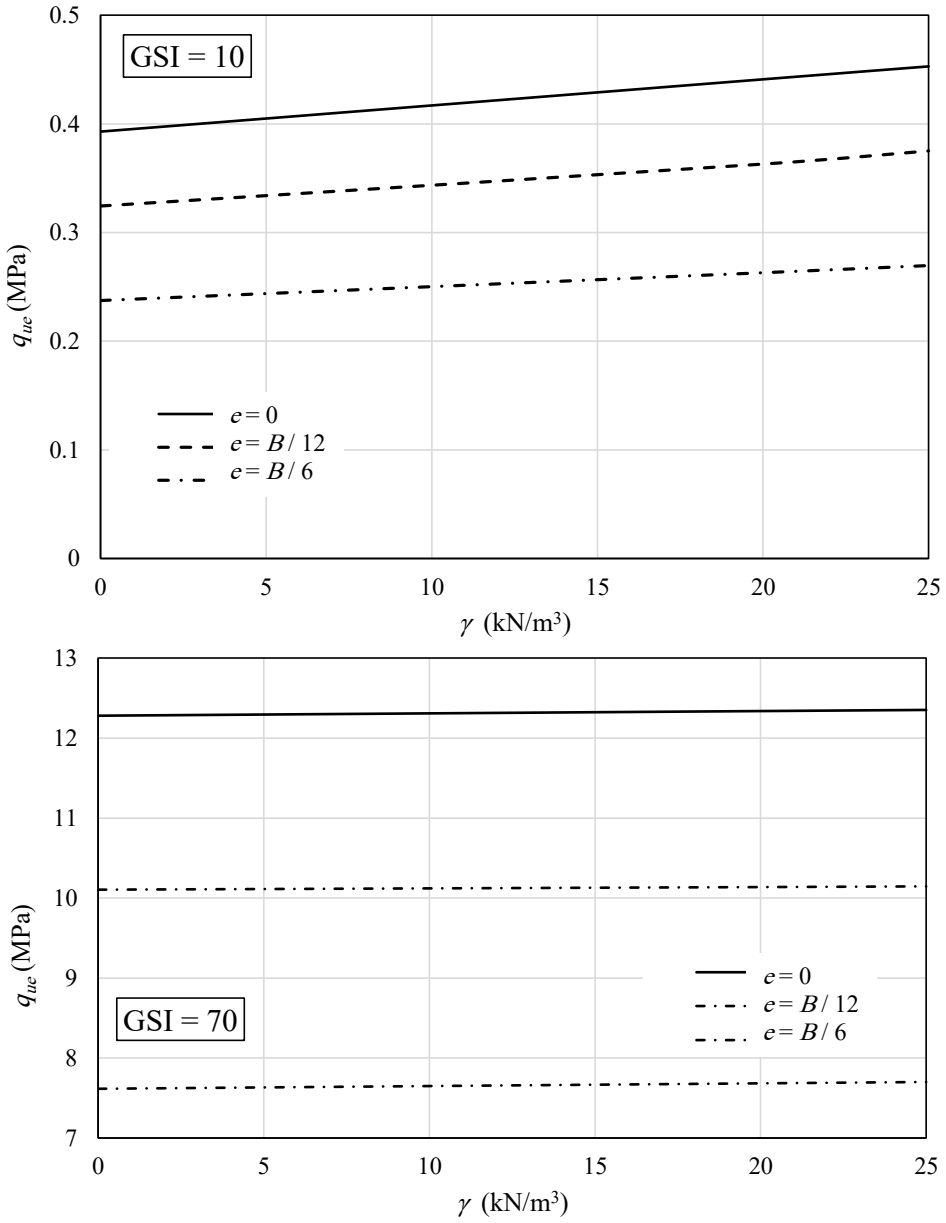

Fig. 11. Variation of q_{ue} versus γ

5- 7- Effect of the rock mass unit weight (γ)

The effect of the rock mass unit weight on the bearing capacity is not considerable and was neglected in most of the previous researches [10, 13, 18, 19, 28]. However, in this section, it was considered under eccentric loads. Ignoring the surcharges, Eq. 14 was used for the analyses. Fig. 11 shows the variation of q_{ue} versus γ by considering different values of e/B and assuming σ_{ci}=10 MPa, m_i=7, and B=1 m. For the cases of GSI=10 and GSI=70, by increasing γ from zero to 25 kN/m^3, the maximum increase in the bearing capacity is about 12.2% and 0.9%, respectively, which shows that for large values of GSI, γ has no significant effect on q_{ue}. It is clear that the eccentricity value does not play a significant role in the effect of γ on q_{ue}. As an example, in the case of GSI=10, by increasing γ from zero to 25 kN/m^3, the q_{ue} increases about 15.2% and 13.5% in the cases of e/B=0 and 0.16, respectively, which shows the slight dependency of q_{ue}-γ variation on the eccentricity.

5- 8- . Effect of surcharge (q)

For studying the effect of q on the bearing capacity, the effect of the rock mass unit weight was neglected. Therefore, Eq. 7, was changed into the following form:

$$q_{ue} = s^{0.5}\sigma_{ci}N_{\sigma e} + qN_{qe} \quad (14)$$

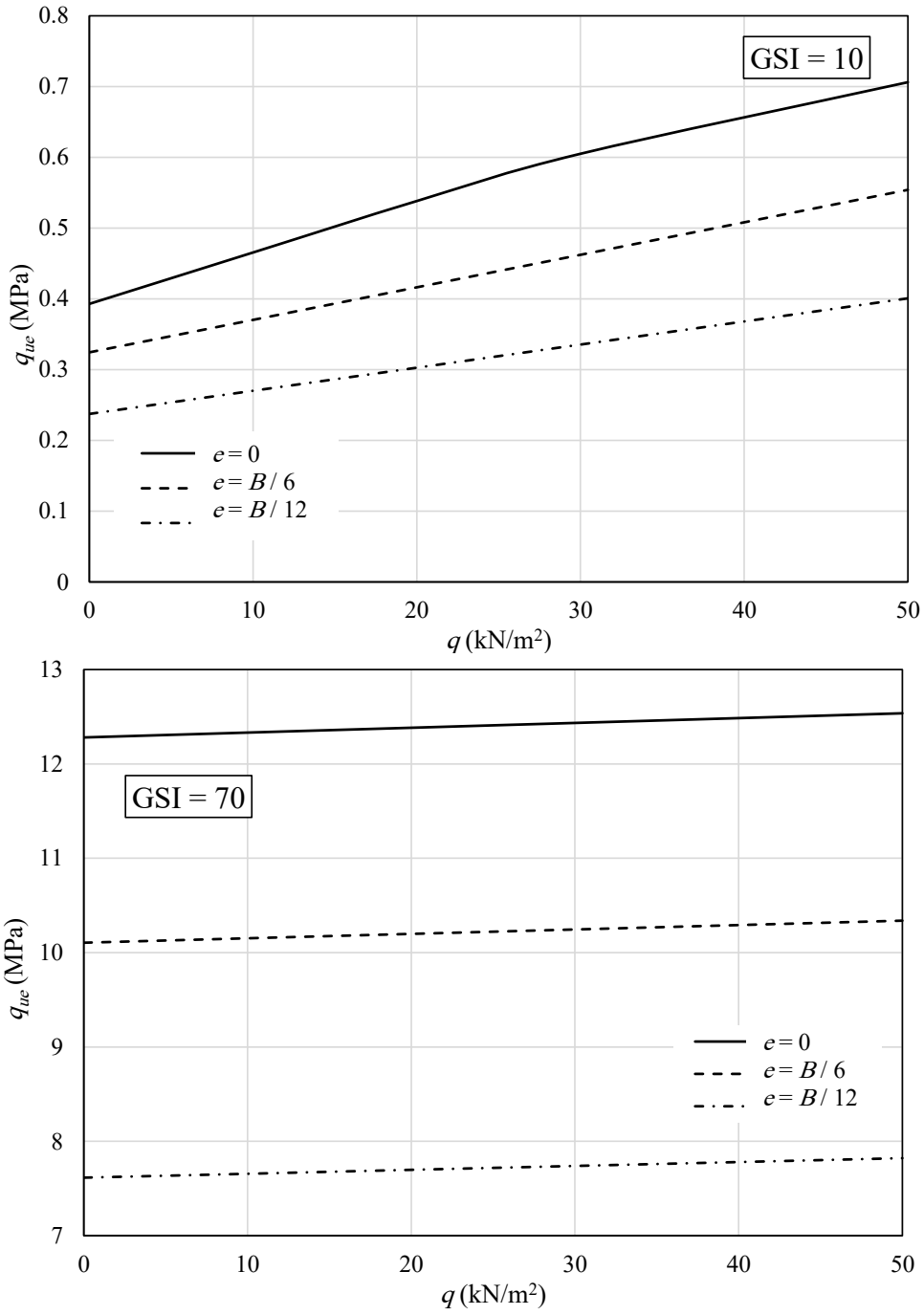

Fig. 12. Variation of q_{ue} versus q

Assuming σ_{ci}=10 MPa, m_i=7, and D=0, the variation of q_{ue} versus q is shown in Fig. 12. In the cases of GSI=10 and 70, by increasing q from zero to 50 kN/m^2, the maximum increase in the bearing capacity is about 79.7% and 2.7%, respectively which shows that for large values of GSI, q has no significant effect on q_{ue}. It is also clear that the role of eccentricity in the q_{ue}-q relationship depends on GSI. For example, in GSI=10, increasing e from zero to B/6 results in increasing the q_{ue} in the range of 66% to 80%, while for GSI=70, the increasing range is between 60% and 61%.

5- 9- Design table

The results of the parametric analyses performed in the present paper is summarized as a design table shown in Table 5. It was assumed that σ_{ci}=10 MPa, D=0, and B=1 m. In practical problems, the ultimate bearing capacity can be obtained by putting the bearing capacity factors $N_{\sigma e}$, N_{qe}, and $N_{\gamma e}$ from Table 4 into Eq. 7.

Table 5. Design table

m_i		7			17		
	GSI	$e = 0$	$e = B/12$	$e = B/6$	$e = 0$	$e = B/12$	$e = B/6$
$N_{\sigma e}$	10	5.832	4.815	3.524	19.376	15.542	11.567
	30	10.977	8.637	6.358	26.595	21.146	15.868
	50	8.469	6.515	5.135	19.762	15.866	11.985
	70	6.502	5.350	4.032	14.012	11.34	8.360
	90	5.931	4.911	3.620	10.079	8.074	6.314
N_{qe}	10	7.263	4.593	3.265	6.620	4.864	3.654
	30	7.324	6.721	4.362	8.097	4.580	3.303
	50	6.689	4.317	4.022	6.674	3.265	2.886
	70	5.107	4.675	4.123	6.910	5.747	5.037
	90	8.121	7.399	5.957	6.629	5.304	5.086
$N_{\gamma e}$	10	4.70	3.789	2.574	4.788	3.327	2.612
	30	4.931	4.852	3.286	5.224	3.800	2.231
	50	4.793	4.601	3.415	4.752	2.946	2.198
	70	6.770	3.301	2.683	4.849	3.710	4.831
	90	4.869	4.322	3.596	4.704	3.686	3.666

6- Conclusion

In summary of the obtained results for different cases considered in the present paper, it is concluded that by increasing the load eccentricity from zero to 1/6 of the footing width, the bearing capacity factor $N_{\sigma e}$ was reduced in the range of 20% to 40%. Also, for all considered eccentricities, the effect of σ_{ci}, m_i, γ, and B on the bearing capacity was reduced by increasing GSI. As a simple conclusion to be used in practical problems, the following variation of $N_{\sigma e}$ can be proposed for the 10<GSI<70. Notably, larger percentages are related to GSI=10, while smaller ones relate to GSI=70.

- By increasing D from zero to 0.5, $N_{\sigma e}$ is reduced within the range of 13 to 20%.
- By increasing m_i from 7 to 25, $N_{\sigma e}$ becomes 2 or 3 times larger.
- Increasing the unit weight of the rock mass from 20 kN/m^3 to 25 kN/m^3 results in increasing the bearing capacity between zero and 15%.
- By increasing the footing width from 1 to 5 meters, the bearing capacity increases between 13% and 46%.
- Increasing the surcharge from zero to 50 kN/m^3, results in increasing bearing capacity up to 79%.
-

References

[1] G. Meyerhof, The ultimate bearing capacity of foudations, Geotechnique, 2(4) (1951) 301-332.

[2] G. Meyerhof, The bearing capacity of foundations under eccentric and inclined loads, in: Proc. of 3rd ICSMFE, 1953, pp. 440-445.

[3] O. Sargazi, E. Seyedi Hosseininia, Bearing capacity of ring footings on cohesionless soil under eccentric load, Computers and Geotechnics, 92 (2017) 169-178.

[4] M. Jao, F. Ahmed, G. Muninarayana, M.C. Wang, Stability of eccentrically loaded footings on slopes, Geomechanics and Geoengineering, 3(2) (2008) 107-111.

[5] B.M. Das, Bearing Capacity of Eccentrically Loaded Surface Footings on Sand, Soils and Foundations, 21(1) (1981) 115-119.

[6] M. Foundoukos, R. Jardine, The effect of eccentric loading on the bearing capacity of shallow foundations, in: BGA International Conference on Foundations: Innovations, observations, design and practice: Proceedings of the international conference organised by British Geotechnical Association and held in Dundee, Scotland on 2–5th September 2003, Thomas Telford Publishing, 2003, pp. 297-305.

[7] S. Saran, R.K. Agarwal, Bearing Capacity of Eccentrically Obliquely Loaded Footing, Journal of Geotechnical Engineering, 117 (1991) 1669-1690.

[8] R.N. Behera, C. Patra, Ultimate Bearing Capacity Prediction of Eccentrically Inclined Loaded Strip Footings, Geotechnical and Geological Engineering, 36(5) (2018) 3029-3080.

[9] M. Imani, A. Fahimifar, M. Sharifzadeh, Effects of Joint Spacing on Static Bearing Capacity of Rock Foundations in the Case of Punching Failure, Amirkabir Journal of Science & Research (Civil & Environmental Engineering), 46(2) (2015) 91-100. (in Persian)

[10] Z. Saada, S. Maghous, D. Garnier, Bearing capacity of shallow foundations on rocks obeying a modified Hoek–Brown failure criterion, Computers and Geotechnics, 35(2) (2008) 144-154.

[11] A. Serrano, C. Olalla, Allowable bearing capacity of rock foundations using a non-linear failure criterium, in: International journal of rock mechanics and mining sciences & geomechanics abstracts, Elsevier, 1996, pp. 327-345.

[12] S. Shamloo, M. Imani, The Effect of Linearization of Hoek-Brown Criterion on the Bearing Capacity of Rock Masses using the Upper Bound Method of Limit Analysis, Amirkabir Journal of Civil Engineering, 54(4) (2022) 1341-1360. (in Persian)

[13] X.-L. Yang, J.-H. Yin, Upper bound solution for ultimate bearing capacity with a modified Hoek–Brown failure criterion, International Journal of Rock Mechanics and Mining Sciences, 42(4) (2005) 550-560.

[14] A. Alencar, R. Galindo, S. Melentijevic, Influence of the groundwater level on the bearing capacity of shallow foundations on the rock mass, Bulletin of Engineering Geology and the Environment, 80 (2021) 6769-6779.

[15] M. Imani, A. Fahimifar, M. Sharifzadeh, Upper bound solution for the bearing capacity of submerged jointed rock foundations, Rock mechanics and rock engineering, 45 (2012) 639-646.

[16] A.H. Javid, A. Fahimifar, M. Imani, Numerical investigation on the bearing capacity of two interfering strip footings resting on a rock mass, Computers and Geotechnics, 69 (2015) 514-528.

[17] A. Javid, A. Fahimifar, M. Imani, Numerical studies on the bearing capacity of two interfering strip footings based on Hoek–brown materials, in: 13th ISRM International Congress of Rock Mechanics, OnePetro, 2015.

[18] S. Shamloo, M. Imani, Upper bound solution for the bearing capacity of two adjacent footings on rock masses, Computers and Geotechnics, 129 (2021) 103855.

[19] H. AlKhafaji, M. Imani, A. Fahimifar, Ultimate bearing capacity of rock mass foundations subjected to seepage forces using modified Hoek–Brown criterion, Rock Mechanics and Rock Engineering, 53 (2020) 251-268.

[20] H. AlKhafaji, M. Imani, A. Fahimifar, Three-Dimensional Bearing Capacity Analysis of Rock Foundations Subjected to the Loads of Gravity Dams, Case Study: Shafaroud Dam, AUT Journal of Civil Engineering, 5(2) (2021) 257-268.

[21] M. Imani, R. Aali, Effects of embedment depth of foundations on ultimate bearing capacity of rock masses, Geotechnical and Geological Engineering, 38 (2020) 6511-6528.

[22] S. Shamloo, M. Imani, Upper bound solution for the bearing capacity of rock masses considering the embedment depth, Ocean Engineering, 218 (2020) 108169.

[23] S. Keawsawasvong, C. Thongchom, S. Likitlersuang, Bearing capacity of strip footing on Hoek-Brown rock mass subjected to eccentric and inclined loading, Transportation Infrastructure Geotechnology, 8 (2021) 189-202.

[24] H. Yousefian, M. Fatehi Marji, H. Soltanian, A. Abdollahipour, Y. Pourmazaheri, Wellbore trajectory optimization of an Iranian oilfield based on mud pressure and failure zone, Journal of Mining and Environment, 11(1) (2020) 193-220.

[25] H.A. Lazemi, M.F. Marji, A.Y. Bafghi, K. Goshtasbi, Rock failure analysis of the broken zone around a circular opening, Archives of Mining Sciences, 58(1) (2013).

[26] W.-F. Chen, Limit analysis and soil plasticity, J. Ross publishing, 2007.

[27] N. Mao, T. Al-Bittar, A.-H. Soubra, Probabilistic analysis and design of strip foundations resting on rocks obeying Hoek–Brown failure criterion, International Journal of Rock Mechanics and Mining Sciences, 49 (2012) 45-58.

[28] M. Mansouri, M. Imani, A. Fahimifar, Ultimate bearing capacity of rock masses under square and rectangular footings, Computers and Geotechnics, 111 (2019) 1-9.

HOW TO CITE THIS ARTICLE

A. Erfanian, M. Imani, Effect of Load Eccentricity on the Bearing Capacity of Strip Footings on Rock Masses, AUT J. Civil Eng., 6(3) (2022) 415-432.

DOI: 10.22060/ajce.2023.22297.5824